Desalination and Water Treatment
www.deswater.com

doi: 10.5004/dwt.2018.22847

130 (2018) 98–108
October

Tyrosinase biosensor based on multiwall carbon nanotubes – titanium oxide nanocomposite for catechol determination

Shadia A. Fathy[a], Fatma F. Abdel Hamid[a], Ahmed El Nemr[b,*], Azza El-Maghraby[c], Eman Serag[a]

[a]*Department of Biochemistry, Faculty of Science, Ain Shams University, Cairo, Egypt, emails: shadiafathy2000@yahoo.com (S.A. Fathy), fatfarag@hotmail.com (F.F. Abdel Hamid), d.emanserag@yahoo.com (E. Serag)*
[b]*Marine Pollution Department, Environmental Division, National Institute of Oceanography and Fisheries, Kayet Bey, Elanfoushy, Alexandria, Egypt, emails: ahmedmoustafaelnemr@yahoo.com, ahmed.m.elnemr@gmail.com*
[c]*Fabrication Technology Department, Advanced Technology and New Materials Institute, City for Scientific Research and Technology Application, Borg El-Arab, Alexandria, Egypt, email: elmaghrabyazza@yahoo.com*

Received 4 January 2018; Accepted 23 July 2018

ABSTRACT

Multiwall carbon nanotubes-titanium oxide nanocomposite (MWCNTs-TiO_2) was formed and used as a conductive material for modification of graphite electrode and tyrosinase immobilization. This nanocomposite showed good conductivity, and biocompatibility with the enzyme. Under optimum conditions, the current response was linear to catechol concentration from 0.2 to 2.7 mM with a sensitivity of 85.79 mA/M and a low detection limit of 0.014 μM, the proposed electrode shows good reproducibility and long-term stability till 25 d. The prepared biosensor was successfully used to measure the catechol in different water samples, with excellent results compared with the spectrophotometric method, at 95% confidence level.

Keywords: MWCNTs-TiO_2; Nanocomposite; Catechol; Tyrosinase; Graphite electrode; Biosensors

1. Introduction

Phenolic compounds are widely distributed in vegetables and fruits [1]. They are also formed in a number of industries such as plastics, dyes, drugs, resins, pesticides, paper, and cellulose industries and released to wastewater streams [2]. Phenol derivatives are known to be highly toxic to humans and to aquatic organisms. They possess immunosuppressive and carcinogenic properties [3,4], and persistent in the environment and highly resistant to biological degradation [1]. As a result, the United States Environmental Protection Agency (EPA) and the European Union (EU) have included these phenolic compounds in their list of primary pollutants [1]. The applications of phenol and its derivatives are considered one of the most potential sources of pollution which affect aquatic organisms, including algae and aquatic spermatophytes [5]. Monitoring these toxic phenols and phenolic derivatives is of great importance in environmental monitoring [6]. Various analytical methods, such as gas chromatography, liquid chromatography, fluorometry, and capillary electrophoresis, have been used for the determination of phenol and its derivatives [1]. Most of these methods are expensive, time consuming, and require professional operators. While, biosensors are considered as suitable tools for real-time detection of phenols in different sample types [5]. Biosensor contains three main parts, the receptor that can identify the target molecules among different chemicals, the transducer that is responsible for the conversion of biorecognition events into electric signals, and an instrument that will record the signals in a readable form [7]. The high selectivity and catalytic activity of enzyme has led to the formation of the electrochemical enzyme biosensor and has become a widely used analytical technique [8].

* Corresponding author.

Enzyme-based amperometric biosensors are suitable for measuring phenolic compounds due to their advantages such as good selectivity, working possibility in aqueous medium, fast responding, relatively low cost of realization and storage and the potential for miniaturization and automation [9]. Amperometric biosensors that have been developed for phenol and its derivatives are usually prepared with working electrode including polyphenol oxidases (tyrosinase and laccase) or enzyme horseradish peroxidase [10].

Tyrosinase is a binuclear copper containing metalloprotein (EC 1.14.18.1). Two consecutive steps involving molecular oxygen are converted to phenols by tyrosinase. Phenol compound is hydroxylated in the first step using molecular oxygen to produce *o*-hydroquinone (catechol), which is named as enzyme's hydroxylase activity (also cresolase activity), and catechol is then oxidized in the second step to an *o*-quinone and, simultaneously, tyrosinase is oxidized by oxygen to its original form with the production of water, and that is known as enzyme's catecholase activity (Fig. 1) [11].

Macholan and Schane reported the analytical role of tyrosinase in biosensor terms by measuring the reduction of oxygen in the determination of phenolic substrates [11]. Since then, tyrosinase-based biosensors have attracted significant attention in the monitoring of phenols, such as catechol, *p*-cresol, and phenol [12].

The key point lies in the immobilization procedure of tyrosinase on a support matrix that binds the enzyme and bare electrode providing efficient electron transport via added functional groups or nanoparticles into the composite structure of the electrode [13]. Otherwise, the quality of the electron transfer between the enzyme redox center and the electrode can be significantly enhanced by using conductive nanoporous structured materials [14].

Carbon nanotube has been applied to construct electrochemical biosensors to improve sensitivity due to its remarkable mechanical, physical, and unique electrochemical properties [5,15,16].

The aim of this study is to prepare nanocomposite materials which have distinct properties and which were not observed in the individual components. The study led to the immobilization of tyrosinase on multiwall carbon nanotubes-titanium oxide nanocomposite (MWCNTs-TiO_2) modified graphite electrode (GE) for detection of catechol in solution and studying the modified electrode quality and accuracy.

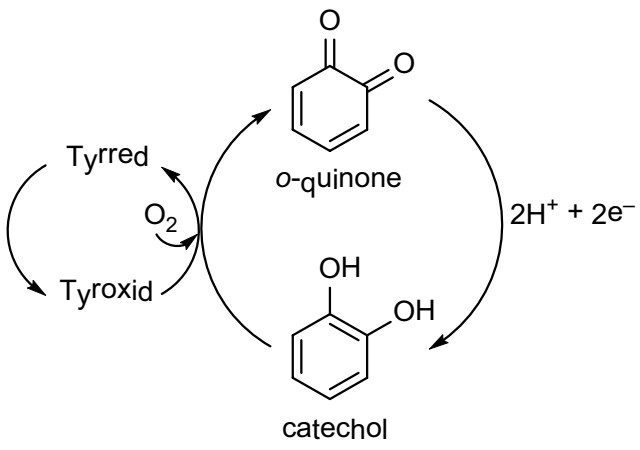

Fig. 1. Scheme of reaction with tyrosinase.

2. Material and methods

2.1. Materials

Aluminum oxide, iron(III) nitrate, cobalt nitrate, and titanium butoxide were obtained from Sigma-Aldrich and were used without further purification. Fresh banana fruits were obtained from the markets for extraction of tyrosinase. Ammonium sulfate, potassium chloride, sodium monohydrogen, and dihydrogen phosphate were purchased from Nasr Co., Egypt and used as received. Catechol (approx. 99%) was purchased from Sigma-Aldrich, USA. GEs (diameter = 8 mm) were from material grade: ST-21, Bay Carbon, INC. (Bay City, MI, USA).

2.2. MWCNT preparation

The MWCNTs was synthesized via chemical vapor deposition (CVD) of Fe_{50}/Co_{50} supported by Al_2O_3 and acetylene as a carbon source. The CVD system consisted of a horizontal quartz reactor (Nabertherm B180-70 cm long, 5.0 cm in diameter) housed in a one-stage cylindrical furnace. The reactor was heated at the rate of 50°C/min to reach the desired temperature under nitrogen gas with flow of 70 mL/min. Acetylene (C_2H_2) was then passed through the reactor tube at the rate of 30 mL/min for 60 min. The flow of gases was controlled by a mass flow controller. Then, the reactor was cooled under a flow of nitrogen (40 mL/min) to room temperature. The grown MWCNT was characterized by scanning electron microscope (SEM).

2.3. MWCNTs oxidation

Pham et al. [17] method was used for the oxidation of MWCNTs as follows: MWCNTs (0.5 g) was dispersed in concentrated H_2SO_4 and HNO_3 (3:1; 80 mL) for 30 min using a sonicator. The mixture was then refluxed at 70°C for 5 h and washed several times with deionized water until the pH reached 7. The carboxylic acid groups functionalized the MWCNTs which was filtered using a 0.2 μm PTFE membrane filter and dried (24 h) at 70°C in a vacuum oven.

2.4. Synthesis of MWCNTs-TiO_2 nanocomposite

The synthesis of MWCNTs-TiO_2 nanocomposite was made according to Haldorai et al. [18]. 0.5 g of oxidized MWCNTs was dispersed in ethanol (250 mL) under sonication, then titanium butoxide (3.0 g) was added to the solution and allowed to mix for 30 min at room temperature, then deionized water (5 mL) was added and allowed to mix for another 30 min, followed by mixture reflux for 6 h and after that the product was filtrated, washed, and annealed under nitrogen at 400°C for 4 h. The nanocomposite obtained was characterized by SEM, Fourier transform infrared (FTIR), and energy dispersive X-ray (EDX).

2.5. Enzyme extraction

20 g of fresh banana pulp were homogenized in the blender in a presence of 0.1 M sodium phosphate buffer (PBS) (pH 7). The homogenate was filtered, combined, and centrifuged at 30,000 rpm for 20 min at 4°C. The supernatant, to be referred to as crude soluble tyrosinase (Tyr) fraction, was stored for further use [19].

2.6. Partial purification of crude enzyme by ammonium sulfate precipitation

Ammonium sulfate precipitation was used as a purification step for the crude soluble tyrosinase. Crude enzyme (20 mL) was taken in a beaker and kept over ice bags (4°C) and ammonium sulfate (45%) was added. The resulting precipitate (partial purified) was dissolved in cold PBS and kept in the refrigerator for further use.

2.7. Assay of enzyme

0.1 mL enzyme extract was added to 2.9 mL of catechol (100 mM) in 0.1 M PBS (pH-7) solution and a change in absorbance at 420 nm was measured using UV-Visible spectrophotometer (UV 3600, Shimadzu, Japan) against reference (3.0 mL catechol). Change in absorbance was recorded every 1 s for 3 min. One unit of Tyr activity was defined as the change in absorbance of 0.001 per minute per milliliter of enzyme. Finally, enzyme activity was 0.187 units/mL. The data were represented as the mean of triplicate measurements [20].

2.8. Measurement of specific activity of enzyme

The protein content of the enzyme was determined by the modified Lowry's method [21] and protein quantity was 1.12 mg/mL using bovine serum albumin as a standard. Specific activity of Tyr was calculated through Eq. (1), and expressed in Units/mg of protein and it was 0.166 U/mg protein.

$$\text{Specific activity}\left(\text{U / mg protein}\right) = \frac{\text{Enzyme activity / mL}}{\text{Protein concentration / mL}} \quad (1)$$

2.9. Fabrication of MWCNT-TiO_2/tyrosinase-modified electrode

The GE surface was polished with 0.3 μm alumina slurries, rinsed thoroughly with deionized water, sonicated in water and acetone, and air dried. 2 mg of MWCNTs-TiO_2 nanocomposite were dispersed in 5 mL of ethanol using ultrasonication for 30 min. 50 μL aliquot of this dispersion was dropped on the GE surface and the solvent was evaporated at ambient temperature. Then, Tyr was immobilized physically by dropping 50 μL aliquot of a partial purified enzyme on the modified electrode surface and letting the solvent evaporate at room temperature. The enzyme-modified electrode was stored in 0.1 M PBS (pH 7) at 4°C when not in use. The modified electrode was characterized by FTIR [22].

2.10. Electrochemical analysis

Cyclic voltammetric (CV) and electrochemical impedance spectroscopy (EIS) measurements were made using a three-electrode system with a potentiostat (Gamry Instruments Electrochemical Analyzer, USA). The auxiliary electrode was graphite, the reference electrode was Ag/AgCl, and the working electrode was graphite modified with MWCNT-TiO_2 nanocomposite and immobilized tyrosinase. All experiments were performed at 25°C ± 2°C, where immobilized tyrosinase had approximately 10°C lower optimum temperature than the free one [23,24].

To demonstrate the practical application of the biosensor for catechol determination in tap water and seawater sample, seawater sample was collected from Al Anfoushy area which is near NIOF institute and was used for quantitative analysis after filtration and pH justified. For unspiked tap water and seawater samples, no catechol was observed by the developed method and the standard spectrophotometric method. To investigate the performance of the proposed biosensor, several known concentrations of catechol (0.2, 0.4, and 0.8 mM) were spiked in tap water and seawater samples and measured using the developed biosensor and spectrophotometric method using standard Folin–Ciocalteu colorimetry [25]. 20 μL of the sample was added into a 2 mL glass cuvette containing 1.58 mL of water. 100 μL FC reagent was added to the cuvette and mixed thoroughly by inverting and then incubated for 5 min. 300 μL Sodium carbonate solution was added, mixed, and incubated for 2 h at room temperature. Absorbance at 765 was read against the blank, and catechol content in the sample was extrapolated from the standard curve between catechol concentration and absorbance 765.

3. Results and discussion

3.1. Characterization of MWCNT-TiO_2 nanocomposite

TiO_2 was deposited on the surface of functionalized MWCNT which act as a nucleating site for growth TiO_2. Annealing was performed at 400°C in the presence of nitrogen gas for 4 h producing MWCNT-TiO_2 nanocomposite. Fig. 2 illustrates the morphology and structure of MWCNT and the nanocomposite. The scanned image shows that the TiO_2 nanoparticles were found to be homogenously deposited on the MWCNTs with minor agglomeration along the MWCNTs [22]. The chemical composition of the MWCNTs-TiO_2 nanocomposite was examined by EDX (Fig. 2(c)). The results confirmed the presence of Ti and O from TiO_2 and C from MWCNTs in the composite.

Fig. 3 shows FTIR of nanocomposite, which is used to investigate the functional groups and the bond between the components in nanocomposite. The peak at 1,556 cm^{-1} is due to the presence of C–O, COO, and C=O on MWCNT after oxidation treatment and the shifting to a lower wave number attributed to a strong binding between COO^- ion on MWCNTs and TiO_2 [26], while the peak was at 1,145 cm^{-1} representing Ti–O–C bond assigned to a covalent link between titanium oxide and MWCNTs [27]. The peaks were at 422, 540, and 635 cm^{-1} representing the anatase phase of titanium oxide and the shifting due to a strong bond between titanium oxide and MWCNT [26].

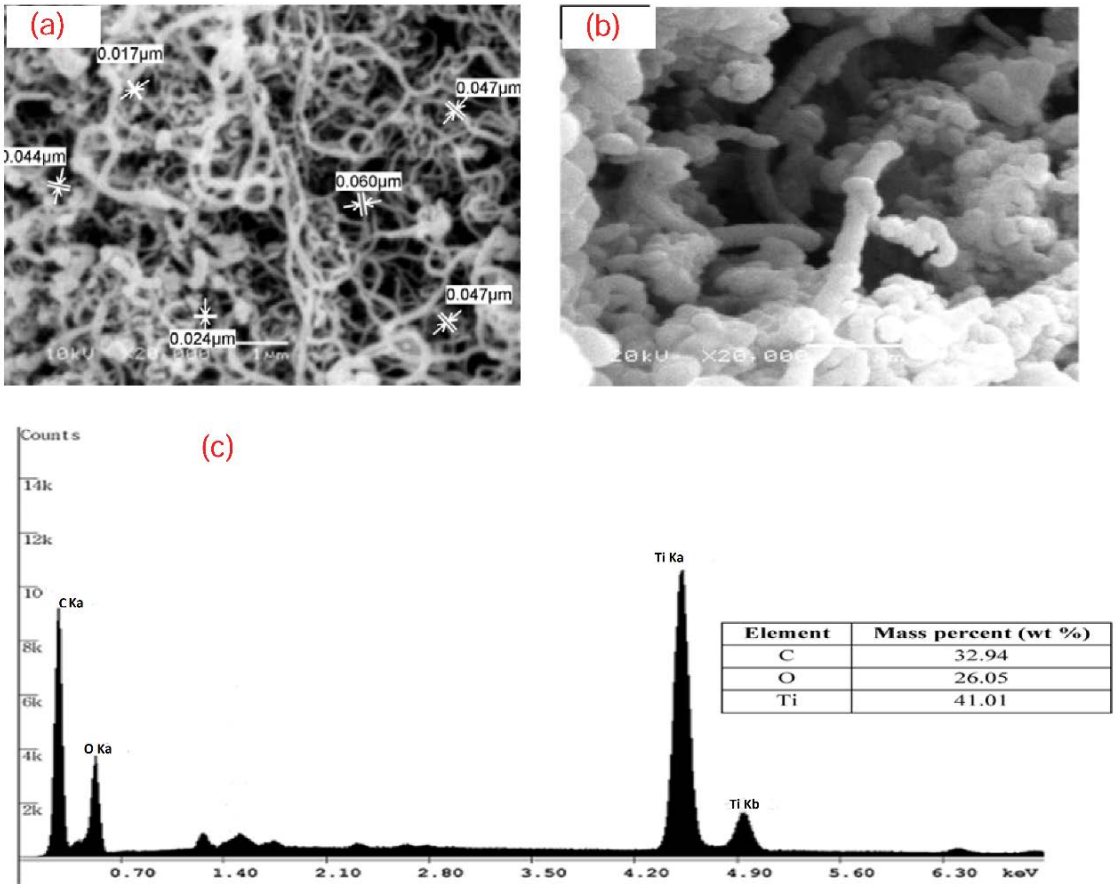

Fig. 2. (a) SEM of as-grown MWCNT, (b) SEM of MWCNT-TiO_2 nanocomposite, and (c) EDX of MWCNT-TiO_2 nanocomposite.

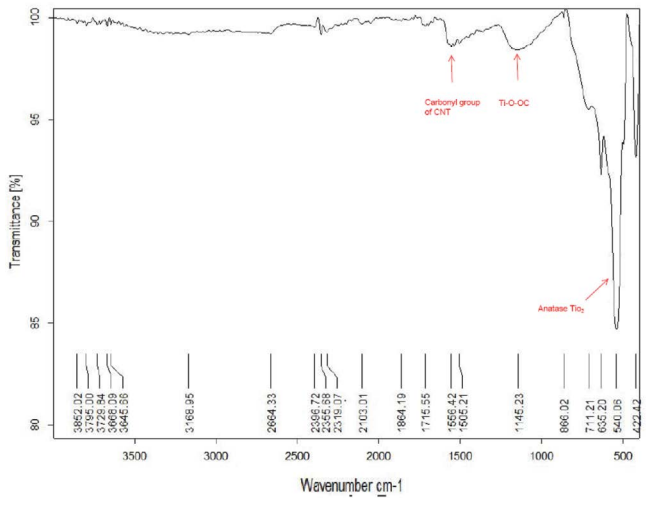

Fig. 3. Fourier transform infrared spectroscope (FTIR) of MWCNT-TiO_2 nanocomposite.

3.2. Intermolecular interaction between MWCNT-TiO_2 and tyrosinase

The interaction between MWCNT-TiO_2 and Tyr was studied by IR spectra (Fig. 4). When Tyr was immobilized on MWCNT-TiO_2 there were some differences in IR spectra between MWCNT-TiO_2/Tyr/GE and MWCNT-TiO_2/GE. The intensity of band at 1,647 cm^{-1} increased due to amide I vibration of Tyr [28]. Otherwise, the band at 1,523 shifted to 1,511 cm^{-1} and its intensity increased. This was attributed to amide II of Tyr [29] and the shifting of the band due to the interaction of Tyr and MWCNT-TiO_2 nanocomposite with the modified GE. There are strong and broad bands between 3,600 and 3,800 cm^{-1} corresponding to O–H, N–H vibrations of Tyr [30].

3.3. Electrocatalytic activity

The electrochemical phenolic biosensors principle is based on the amperometric detection of *o*-quinone as the enzymatic product that is generated from the oxidation of catechol by Tyr as catalysis in the presence of dissolved oxygen. Thus, the reduction current of the *o*-quinone is measured in the current work by the amperometric response, and is used to indirectly measure the concentration of phenolic compounds [5]. The enzymatic reaction steps on the bioelectrode surface are shown in Fig. 5.

Fig. 6(a) represents the cyclic voltammogram (CVs) responses of MWCNTs/Tyr/GE, and MWCNTs-TiO_2/Tyr/GE electrodes in 0.1 M KCl containing 0.1 mM of $Fe(CN)_6^{3-/4-}$ redox couple (ferricyanide was chosen as a marker to investigate the behaviors of different electrodes) in a potential range –0.2 to 1.2 V. It was observed that there was an

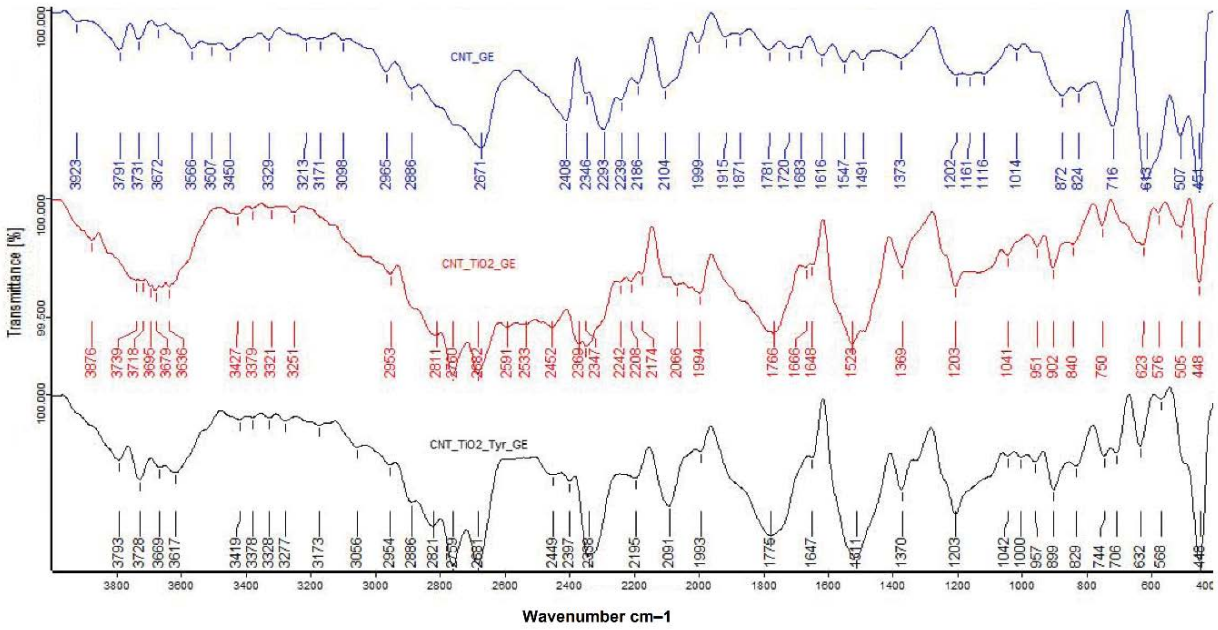

Fig. 4. FTIR of the modified electrodes.

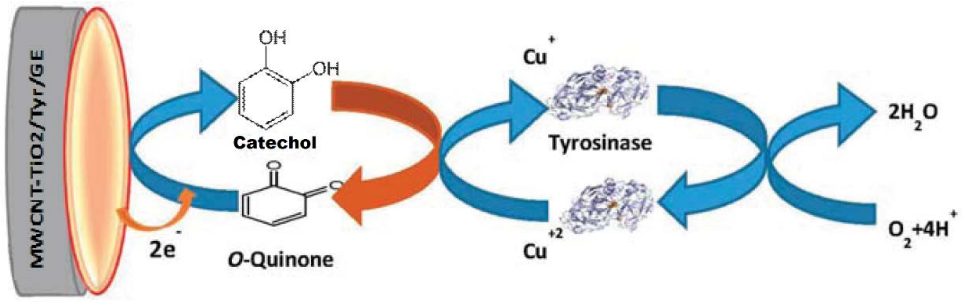

Fig. 5. Possible mechanisms occur on the surface of electrode.

enhancement in redox peaks for MWCNTs-TiO_2/Tyr/GE. This was attributed to the fact that the current was enhanced when TiO_2 nanoparticles coupled with MWCNT as a MWCNT-TiO_2 nanocomposite-modified electrode, and these results were similar to those reported earlier [22]. Ipa/Ipc for MWCNT/Tyr/GE, MWCNT-TiO_2/Tyr/GE electrodes are close to 1, confirming the reversibility of the electrode.

To understand the kinetics of the electron transfer process at the MWCNTs-TiO_2/Tyr/GE (Fig. 6(b)), CVs of the electrode in 0.1 M KCl containing 0.1 mM $Fe(CN)_6^{3-/4-}$ solution were performed at scan rates from 20 to 70 mV/s. The anodic/cathodic peak positions shifted gradually with the increase of the scan rate and the separation between anodic and cathodic peaks increased. The anodic peak current showed a linear increase with the increase of the scan rate, indicating a surface-controlled electrode process [31].

3.4. Response toward catechol at the MWCNT-TiO_2/Tyr electrode

To evaluate the catalytic activity of Tyr at the modified electrodes, it was characterized by a cyclic voltammogram in the presence of catechol in the potential range from –0.2 to 1 V. Fig. 7(a) shows CVs of different electrodes in 0.1 M PBS (pH = 7) at 25 mV/s. Ipa of MWCNT-TiO_2/Tyr/GE was higher than that of MWCNT/Tyr/GE, and this indicates that MWCNT-TiO_2 is a good support matrix for Tyr immobilization; furthermore, the presence of TiO_2 with MWCNT in a composite improved the electrocatalysis and enhanced the response signals of modified electrode by facilitating the electron transfer between catechol and the electrode.

Fig. 7(b) shows the CVs of the MWCNTs-TiO_2/Tyr/GE in 0.1 M PBS (pH 7) recorded at different scan rates (20–60 mV/s). The cathodic and anodic peak currents showed linear increase with scan rates indicated that the electrode reaction of Tyr immobilized onto the MWCNTs-TiO_2 nanocomposite corresponded to the process of surface-controlled. When the scan rate increased, the oxidation potential of Tyr for direct electron transfer shifted to a more positive potential, while the reduction peak potential shifted to a more negative value as well as the anodic/cathodic peak separation increased with the scan rate increased.

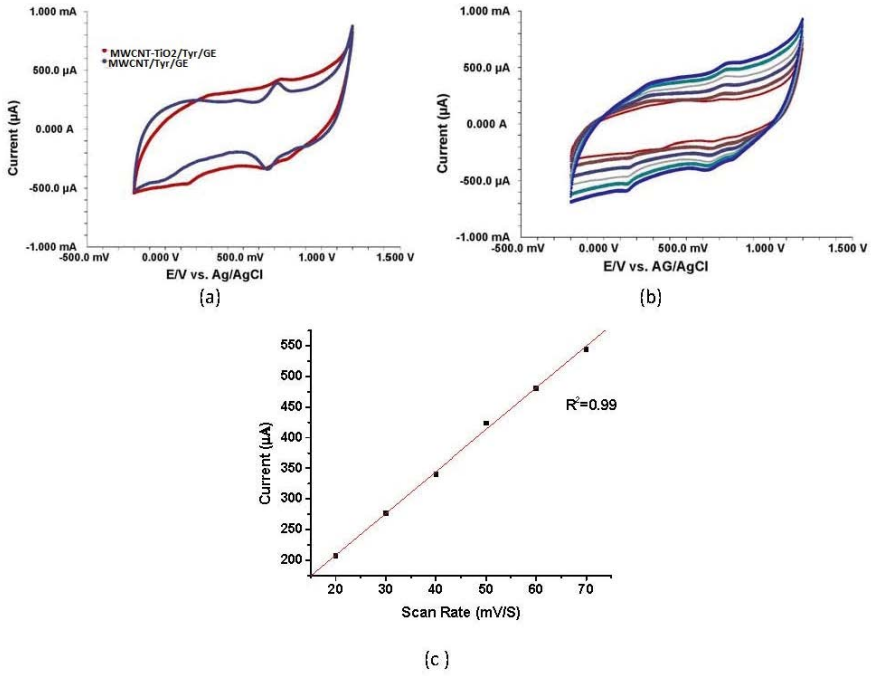

Fig. 6. (a) CVs of different electrodes in 0.1 M KCl containing 0.1 mM of ferro–ferricyanide solution at a scan rate of 25 mV/s; (b) CVs of the MWCNTs-TiO_2/Tyr/GC electrode in 0.1 M KCl containing 0.1 mM $K_3Fe(CN)_6/K_4Fe(CN)_6$ solution at various scan rates (from 20 to 70 mV/s); (c) a plot of the Ipa against scan rate.

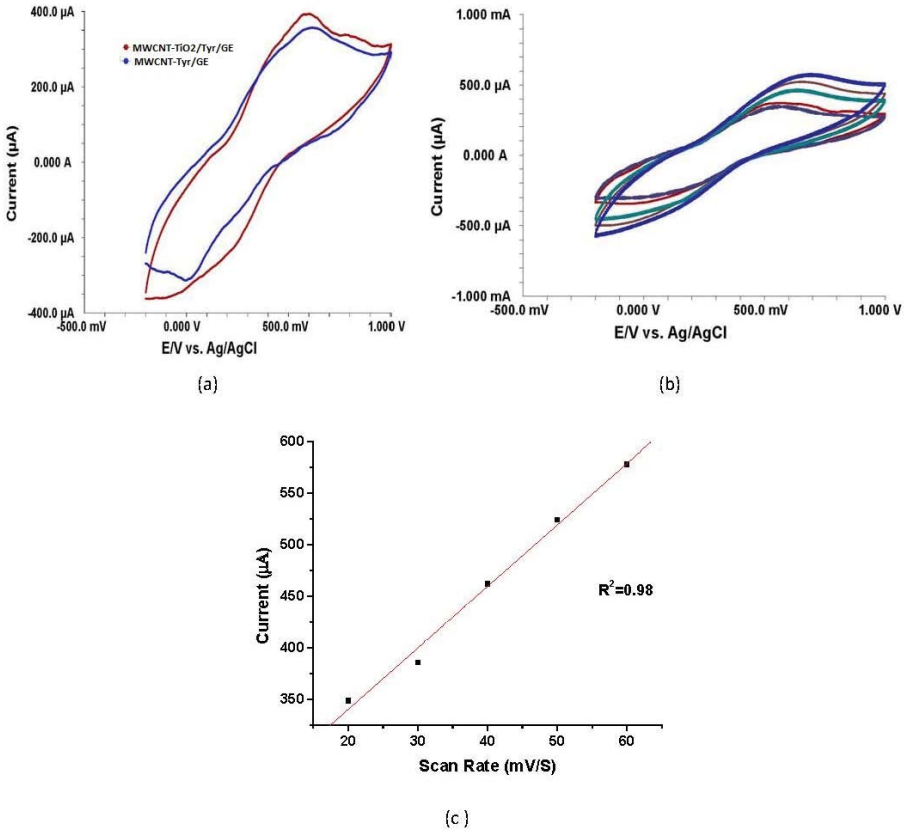

Fig. 7. (a) CVs of different electrodes in 0.1 M PBS (pH 7) in presence of 2.5 mM catechol at scan rate of 25 mV/s; (b) CVs of MWCNT-TiO_2/Tyr/GE in PBS (pH 7) in presence of 2.5 mM catechol at various scan rates 20, 30, 40, 50, and 60 mV/s; (c) the plot of the anodic peak current versus the potential scan rate.

3.5. Electrochemical impedance spectroscopy

EIS is a significant technique to detect changes occurring on the surfaces of biosensor [7]. In Nyquist plots (Fig. 8), it was seen that the electron transfer resistance (R_{et}) for MWCNT-modified GE was 78.42 Ω, while the R_{et} of MWCNT-TiO_2-modified GE was 19.35 Ω, and this was attributed to TiO_2 belonging to semiconductors, which increased the conductivity of nanocomposite [32]. The value of R_{et} increased to 94.28 Ω for MWCNT-TiO_2/Tyr/GE and this may be due to the low conductivity of the Tyr, which slowed the redox reaction of $[Fe(CN)_6]^{3-/4-}$; otherwise, this indicates that Tyr was successfully immobilized onto the GCE modified with MWCNT-TiO_2 [12,25].

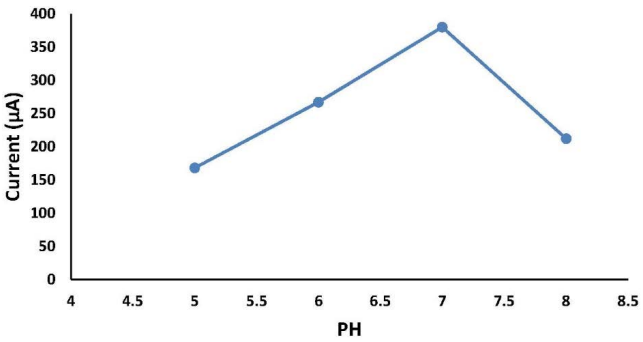

Fig. 9. Effect of pH on the peak current.

3.6. Effect of pH on the determination of catechol

The effect of pH on the current response of the MWCNT-TiO_2/Tyr/GE biosensor was evaluated in the presence of 2.5 mM catechol solution in a 0.1 M PBS at a scan rate 25 mV/s. Since the literature reports that free Tyr loses activity irreversibly below pH 4.5 and above pH 9 [9], the selected pH range was from 5.0 to 8.0. As seen in Fig. 9, the intensity of currents increased with the increase in pH up to 7.0 and started to decrease above pH 7.0. The increase in peak current with increase in pH value from 5 to 7 is due to improvement in Tyr activity as the hydroxyl groups of catechol were binding with copper atoms of the binuclear center of Tyr [29]. While at pH higher than 7 the peak current decrease due to denaturation of the enzyme and this result is similar to that reported previously [33]. Therefore, the phosphate buffer solution (pH 7.0) was used as supporting electrolyte in this study.

3.7. Effect of catechol concentrations

The relationship between the catechol concentrations and the anodic peak current of the biosensor in 0.1 M PBS (pH 7) (calibration curve) is shown in Fig. 10(a). From the Fig. 10(a), it can be seen that the response current is linear with catechol concentrations in the range from 0.2 to 2.7 mM following the equation $y = 157 + 85.79C$ with R^2 value equals 0.964.

3.8. Michaelis–Menten analysis (Lineweaver–Burkplots)

A modified version of the Michaelis–Menten Eq. (2) states that

$$ip^{-1} = i_{\max}^{-1} + \left(K_m \times i_{\max}^{-1}\right)[C]^{-1} \quad (2)$$

where $i_{\max}$ is the maximum current at saturated substrate concentration, and C is the concentration of substrate in mM, and K_m is the constant of Michaelis–Menten, which is calculated by dividing the slope of line by its y-intercept ($i_{\max}^{-1}$) [14]. The linear regression analysis for the catechol is $ip^{-1} = 0.00282 + 6.872 \times 10^{-4}$ with R^2 values of 0.9834 (Fig. 10(b)). The K_m obtained for catechol was 4.11 mM, which is lower than that of MWCNT-titania-Nafion [34].

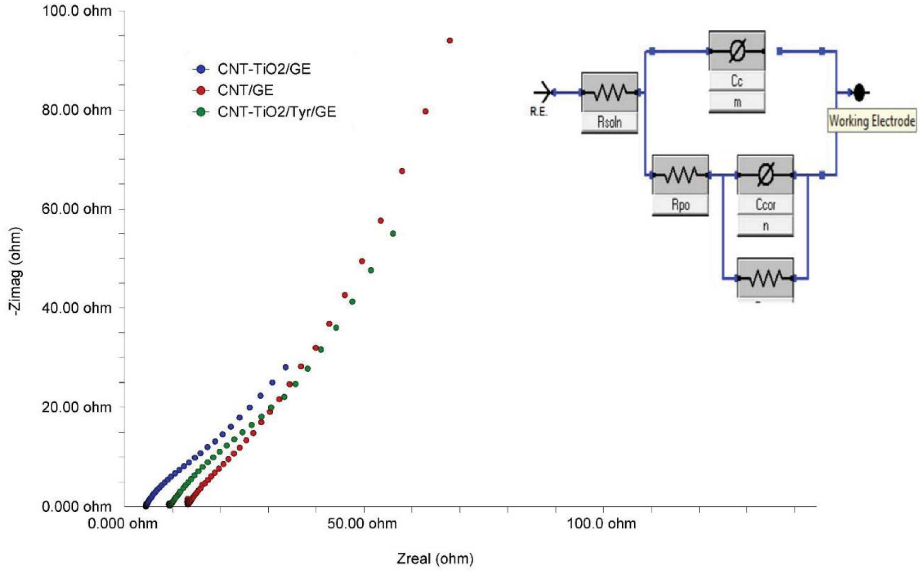

Fig. 8. The Nyquist plots for MWCNT/GE, MWCNT-TiO_2/GE, and MWCNT-TiO_2/Tyr/GE in the presence of 0.1 M KCl solution containing 0.1 mM $K_3Fe(CN)_6/K_4Fe(CN)_6$ applying an AC voltage with 10.0 mV amplitude at a frequency range of 0.2 to 1.0×10^5 Hz.

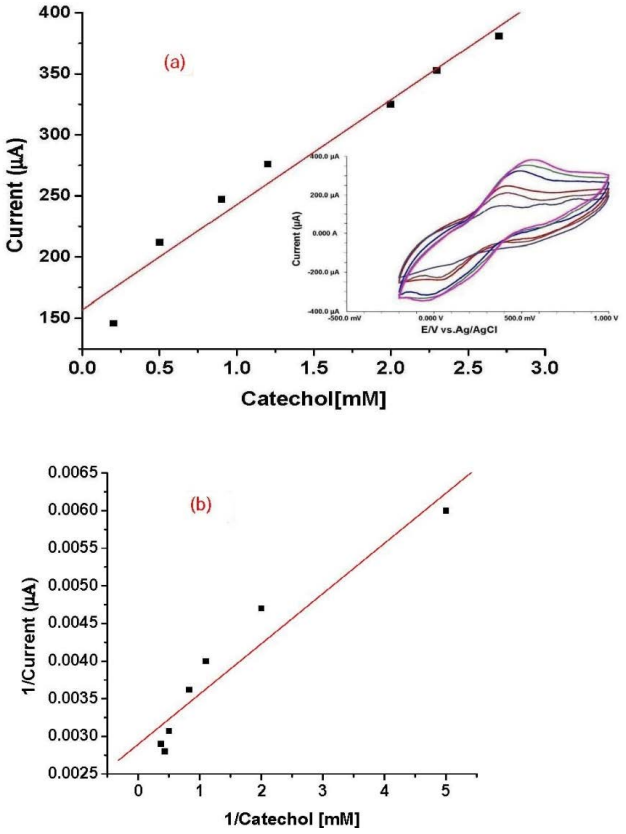

Fig. 10. (a) Calibration plot of catechol at the MWCNTs-TiO_2/Tyr/GE in 0.1 M PBS (pH 7), (b) Line weaver–Burk plot.

The detection limit was calculated as 0.014 mM (three times of the standard deviation for the blank solution (n = 3) divided by the analytical curve slope), and its sensitivity was 85.7 μA/mM, the high sensitivity of the biosensor can be attributed to the porous nature of the MWCNT [34]. These results were comparable with those reported in the literature (Table 1).

3.9. The performance of MWCNT-TiO_2/Tyr biosensor

3.9.1. Interference studies

The selectivity of the MWCNT-TiO_2/Tyr/GE was tested by measuring its response via cyclic voltammetry to some organic materials such as vanillic acid, and salicylic acid, whose structure are similar to catechol, also ascorbic acid and H_2O_2 which acts as Tyr inhibitor, otherwise minerals like Mg^{2+}, Fe^{3+}, and Ca^{2+} may act as competitor inhibitors to Tyr active site. The response currents were obtained by adding the interferents into 0.1 M PBS (pH 7.0) containing 0.2 mM of catechol, and the ratio of interferents to catechol was 1:1 [4]. First of all, the current value of PBS with 0.2 mM of catechol was recorded as I_c. Then, the current value of each solution containing interferents was marked as I_i. At last, the percentage of the interference current value for the catechol current value ($I_i/I_c \times 100\%$) was shown in Fig. 11. It was observed that there was no significant change in the current response in the presence of vanillic acid, salicylic acid, Mg^{2+}, and Ca^{2+}, while ascorbic acid and Fe^{2+} caused some interference. This might be related to ascorbic acid being one of the enzyme inhibitors, which might reduce the Tyr activity [35].

3.9.2. Repeatability, reproducibility, and shelf life of biosensor

To evaluate the repeatability of the MWCNTs-TiO_2/Try/GE electrode, 15 cycles of CVs were carried out using 0.2 mM of catechol in 0.1 M PBS. The plot of the anodic peak current versus its number of cycles (Figs. 12(a) and (b)) showed that the peak current fell by 8.7% during 15 cycles, represents the high stability of the electrode. The reproducibility of the biosensor was demonstrated via measurement of the CV peak current changes (Fig. 12(c)) of five different electrodes during the detection of 0.2 mM of catechol. The relative standard deviation (RSD) was calculated as 1.18%, indicating the good reproducibility of the electrode. The shelf life of MWCNT-TiO_2/Tyr/GE, stored at PBS pH 7 at 4°C, was tested for up to 25 d by monitoring the peak current produced by 0.2 mM

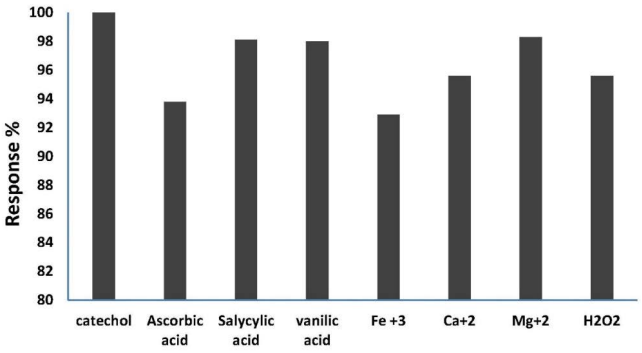

Fig. 11. Interference test of the electrode with 0.2 mM catechol in the presence of various interferents.

Table 1
Comparison between MWCNT-TIO_2/Tyr biosensor and other tyrosinase biosensor for catechol determination

Electrode	Linear range	Low detection limit	Sensitivity	Reference
Tyr-IL-MWCNT-DHP/GCE	4.9–1,100 μM	0.58 μM	32.8 mA/M	[11]
Tyr-PAPCP/ITO	1.6–140 μM	1.2 μM	–	[35]
Agarose-guar gum entrapped tyrosinase	60–800 μM	6 μM	–	[36]
Tyr-MWCNT-MNP/SPE	10–80 μM	7.6 μM	4.8 mA/M	[37]
MWCNT-TiO_2^-/Tyr/GE	0.2–2.7 mM	0.014 mM	85.7 mA/M	This work

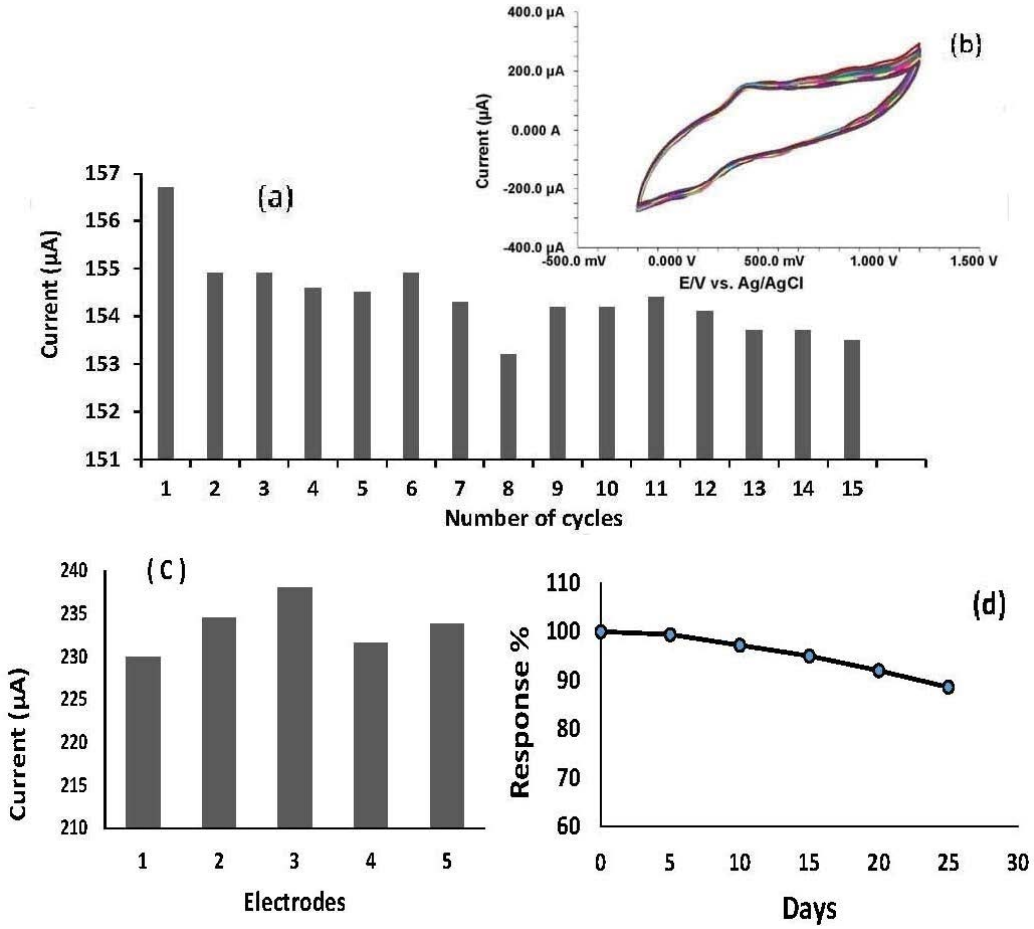

Fig. 12. (a) CVs of the MWCNTs-TiO_2/Tyr/GE for 15 multiple cycles to detect 0.2 mM catechol at a scan rate of 25 mV/s; (b) anodic peak current of the MWCNTs-TiO_2/Tyr/GE for 15 multiple cycles to detect 0.2 mM catechol at a scan rate of 25 mV/s; (c) anodic peak currents of five different MWCNTs-TiO_2/Tyr/GE to detect 0.2 mM catechol at a scan rate of 25 mV/s, and (d) shelf life of the MWCNTs-TiO_2/Tyr/GE after 25 d.

catechol solution every 3–5 d. The biosensor showed a stable response up to 25 d with an RSD of around 5.17% (Fig. 12(d)). The stability of this biosensor during this working period was higher than the biosensor with other complex matrices such as Fe_3O_4 MNPs-CNTs/Tyr [38] and TiO_2/CeO_2/Tyr [39] and this is related to the good entrapment of the enzyme within the MWCNT-TiO_2 matrix as well as the good chemical stability of nanocomposite.

3.9.3. Real sample analysis

To demonstrate the practical application of the biosensor for catechol determination in tap water and seawater sample, seawater sample was collected from Al Anfoushy area which is near NIOF institute and was used for quantitative analysis after filtration and pH justified. For unspiked tap water and seawater samples, no catechol was observed by the developed method and the standard spectrophotometric method. To investigate the performance of the proposed biosensor, several known concentrations of catechol (0.2, 0.4, and 0.8 mM) were spiked in tap water and seawater samples and measured using the developed biosensor and spectrophotometric method.

For each sample, three determinations were performed, and the standard deviations were reported (Table 2). The results obtained by both methods were subjected to the paired *t*-test [11] and the *t* value calculated (1.65) was lower than the critical value (2.015, $p = 0.05$). Therefore, we can conclude

Table 2
Determination of catechol in water samples using the MWCNT-TiO_2/Tyr/GE biosensor and spectrophotometric method

Sample	Catechol added	Catechol concentration (mM) by biosensor (means ± SD, $n = 3$)	Catechol concentration (mM) by spectrophotometer (means ± SD, $n = 3$)
Seawater 1	0.2 mM	0.22 ± 0.014	0.23 ± 0. 0122
Seawater 2	0.4 mM	0.42 ± 0.0104	0.42 ± 0.01
Seawater 3	0.8 mM	0.86 ± 0. 0143	0.85 ± 0.011
Tap water 1	0.2 mM	0.23 ± 0.016	0.24 ± 0.013
Tap water 2	0.4 mM	0.42 ± 0.01	0.42 ± 0.02
Tap water 3	0.8 mM	0.83 ± 0.022	0.85 ± 0.012

that there was no difference between the two methods at a confidence level of 95%. This demonstrates that MWCNT-TiO_2/Tyr/GE biosensor is appropriate for the determination of catechol in water samples.

4. Conclusion

In this study, Tyr enzyme was successfully immobilized in MWCNT-TiO_2/GE. The use of MWCNT and TiO_2 in a nanocomposite increased the conductivity, electrocatalytic activity as well as the analytical signal. The MWCNT-TiO_2/Tyr/GE biosensor was applied to determine catechol by a simple and inexpensive method with linear range from 0.2 to 2.7 mM and a detection limit of 0.014 μM, exhibiting high stability and long lifetime. The MWCNT-TiO_2/Tyr/GE biosensor was applied to determine the catechol in tap water and seawater samples with good results. Moreover, the application of the proposed biosensor may be an acceptable methodology to immobilize other enzymes or proteins.

References

[1] N. Negash, H. Alemu, M. Tessema, Determination of phenol and chlorophenols at single-wall carbon nanotubes/poly (3,4-ethylenedioxythiophene) modified glassy carbon electrode using flow injection amperometry, Int. Sch. Res. Notices, 4 (2014) 59246–459257.

[2] F.C. Vicentini, L.L.C. Garcia, L.C.S. Figueiredo-Filho, B.C. Janegitz, O. Fatibello-Filho, A biosensor based on gold nanoparticles, dihexadecylphosphate, and tyrosinase for the determination of catechol in natural waters, Enzyme Microb. Technol., 84 (2016) 17–23.

[3] R.S. Freire, N. Dur, Electrochemical biosensor-based devices for continuous phenols monitoring in environmental matrices. J. Braz. Chem. Soc., 13 (2002) 456–462.

[4] H.B. Yildiz, J. Castillo, D.A. Guschin, L. Toppare, W. Schuhmann, Phenol biosensor based on electrochemically controlled integration of tyrosinase in a redox polymer, Microchim. Acta, 159 (2007) 27–34.

[5] B. Wang, J. Zheng, Y. He, Q. Sheng, A sandwich-type phenolic biosensor based on tyrosinase embedding into single-wall carbon nanotubes and poly aniline nanocomposites, Sens. Actuators, B, 186 (2013) 417–422.

[6] A.C. Pereira, A. Kisner, C.T.T. Ricardo, N. Duran, L.T. Kubota, Determination of phenol compounds based on electrodes with HRP immobilized on an oxidized multiwall carbon nanotube, Dyn. Biochem. Process Biotechnol. Mol. Biol., Special Issue, 2 (2009) 75–79.

[7] J. Yang, D. Li, J. Fu., F. Huang, Q. Wei, TiO_2-CuCNFs based laccase biosensor for enhanced electrocatalysis in hydroquinone detection, J. Electroanal. Chem., 766 (2016) 16–23.

[8] S.V. Dzyadevych, V.N. Arkhypova, A.P. Soldatkin, A.V. El'skaya, C. Martelet, N. Jaffrezic-Renault, Amperometric enzyme biosensors: past, present and future, IRBM, 29 (2008) 171–180.

[9] I. Gul, M.S. Ahmad, S.M.S. Naqvi, A. Hussain, R. Wali, A.A. Farooqi, I. Ahmed, Polyphenol oxidase (PPO) based biosensors for detection of phenolic compounds: a review, J. Appl. Biol. Biotechnol., 5 (2017) 72–85.

[10] M.M. Rodríguez-Delgado, M. Melissa, G.S. Alemán-Nava, M. José, D. Graciano, S.O. Martínez-Chapa, B. Damià, P. Roberto, Laccase-based biosensors for detection of phenolic compounds, Trends Anal. Chem., 74 (2015) 21–4.

[11] F.C. Vicentini, B.C. Janegitz, C.M.A. Brett, O. Fatibello-Filho, Tyrosinase biosensor based on a glassy carbon electrode modified with multi-walled carbon nanotubes and1-butyl-3-methylimidazolium chloride within a dihexadecylphosphate film, Sens. Actuators, B, 188 (2013) 1101–1108.

[12] L. Tang, Y. Zhou, G. Zeng, Z. Li, Y. Liu, Y. Zhang, G. Chen, G. Yang, X. Lei, M. Wu, A tyrosinase biosensor based on ordered mesoporous-carbon–Au/L-lysine/Au nanoparticles for simultaneous determination of hydroquinone and catechol, Analyst, 138 (2013) 3552–3560.

[13] Y. Haldorai, S.K. Hwang, A.I. Gopalan, Y.S. Huh, Y.K. Han, W. Voit, G. Sai-Anand, K.P. Lee, Direct electrochemistry of cytochrome c immobilized on titanium nitride/multi-walled carbon nano tube composite for amperometric nitrite biosensor, Biosens. Bioelectron., 79 (2016) 543–552.

[14] A. Mohammadi, A.B. Moghaddam, R. Dinarvand, S.R. Zarchi, Direct electron transfer of polyphenol oxidase on carbon nanotube surfaces: application in biosensing, Int. J. Electrochem. Sci., 4 (2009) 895–905.

[15] J. Wang, R.P. Deo, M. Musameh, Stable and sensitive electrochemical detection of phenolic compounds at carbon nanotube modified glassy carbon electrodes, Electroanalysis, 15 (2003) 1830–1834.

[16] E.R. Sartori, F.C. Vicentini, O. Fatibello-Filho, Indirect determination of sulfite using a polyphenol oxidase biosensor based on a glassy carbon electrode modified with multi-walled carbon nanotubes and gold nanoparticles within a poly(allylamine hydrochloride) film, Talanta, 87 (2011) 235–242.

[17] Q.L. Pham, Y. Haldorai, V.H. Nguyen, D. Tuma, J.J. Shim, Facil synthesis of poly(p-phenylendiamin)/MWCNT nanocomposite and characterization for investigation of structural effects of carbon nanotubes, Bull. Mater. Sci., 34 (2011) 37–43.

[18] Y. Haldorai, A. Rengaraj, J.-B. Lee, Y.S. Huh, Y.-K. Han, Highly efficient hydrogen production via water splitting using MWCNT/TiO_2 ternary hybrid composite as a catalyst under UV-Visible light, Synth. Met., 199 (2015) 345–352.

[19] P. Velichkova, D. Marinkova, S. Yaneva, L. Yotova, Isolation and Purification of Tyrosinase from Different Plant Sources, First National Conference of Biotechnology, vol. 100, 2014, pp. 70–75.

[20] M. Alamelumangai, J. Dhanalakshmi, M. Mathumitha, R.S. Renganayaki, P. Muthukumaran, N. Rajalakshmi, Modulation of banana polyphenol oxidase (PPO) activity by naturally occurring bioactive compounds from plant extracts, Int. J. Pharm. Sci. Res., 6 (2015) 41–44.

[21] T. Ohnishi, J. Parr, Protein measurement with the folin reagent, J. Anal. Biochem., 86 (1978) 193–200.

[22] G. Perenlei, T. Wee Tee, N.Z. Yusof, G.J. Kheng, Voltammetric detection of potassium ferricyanide mediated by multi-walled carbon nanotube/titanium dioxide composite modified glassy carbon electrode, Int. J. Electrochem. Sci., 6 (2011) 520–531.

[23] D. Wojcieszyńska, K. Hupert-Kocurek, U. Guzik, Influence of the entrapment of catechol 2,3-dioxygenase in κ-Carrageenan on its properties, Pol. J. Environ. Stud., 22 (2013) 1219–1225.

[24] L. Donato, C. Algieri, A. Rizzi, L. Giorno, Kinetic study of tyrosinase immobilized on polymeric membrane, J. Membr. Sci., 454 (2014) 346–350.

[25] R. Rawal, S. Chawla, C.S. Pundir, Polyphenol biosensor based on laccase immobilized onto silver nanoparticles/multiwall carbon nanotube/polyaniline gold electrode, Anal. Biochem., 419 (2011) 196–204.

[26] V.K. Gupta, T.A. Saleh, Synthesis of Carbon Nanotube-Metal Oxides Composites; Adsorption and Photo-Degradation, Chapter 17 of Carbon Nanotubes - From Research to Applications, In Tech Publisher, 2011, pp. 295–312.

[27] E.T. Mombeshoraa, R. Simoyia, V.O. Nyamoria, P.G. Ndungu, Multiwalled carbon nanotube-titania nanocomposites: understanding nano-structural parameters and functionality in dye-sensitized solar cells, S. Afr. J. Chem., 68 (2015) 153–164.

[28] F.A. Abd Manan, J. Abdullah, N.N. Nazri, I.N. Abd Malik, N.A. Yusof, I. Ahmad, Immobilization of tyrosinase in nanocrystalline cellulose/chitosan composite film for amperometric detection of phenol, Malaysian J. Anal. Sci., 20 (2016) 978 – 985.

[29] F.M. Fartas, J. Abdullah, N.A. Yusof, Y. Sulaiman, M.I. Saiman, Biosensor based on tyrosinase immobilized on graphene-decorated gold nanoparticle/chitosan for phenolic detection in aqueous, Sensors, 17 (2017) 1132–1146.

[30] G. Wang, J.-J. Xu, L.H. Ye, J.J. Zhu, H.Y. Chen, Highly sensitive sensors based on the immobilization of tyrosinase in chitosan, Bioelectrochemistry, 57 (2002) 33– 38.
[31] N.M. Ahmad, J. Abdullah, N.Z. Yusof, A.H. Ab Rashid, S. Abd Rahman, M.R. Hassan, Amperometric biosensor based on zirconium oxide/polyethylene glycol/tyrosinase composite film for the detection of phenolic compounds, Biosensors, 6 (2016) 31–45.
[32] M. Romero-Arcos, M.G. Garnica-Romo, H.E. Martínez-Flores, Electrochemical study and characterization of an amperometric biosensor based on the immobilization of laccase in a nanostructure of TiO_2 synthesized by the sol-gel method, Materials, 9 (2016) 543–555.
[33] B.C. Janegitz, R.A. Medeiros, R.C. Rocha-filho, O. Fatibello-filho, Diamond and related materials direct electrochemistry of tyrosinase and biosensing for phenol based on gold nanoparticles electrodeposited on a boron-doped diamond electrode, Diamond Relat. Mater., 25 (2012) 128–133.
[34] Y. Lee, Y.K. Lyu, H.N. Choi, W.Y. Lee, Amperometric tyrosinase biosensor based on carbon nanotube-titania–nafion composite film, Electroanalysis, 19 (2007) 1048–1054.
[35] Rajesh, W. Takashima, K. Kaneto, Amperometric phenol biosensor based on covalent immobilization of tyrosinase onto an electrochemically prepared novel copolymer poly(N-3-aminopropyl pyrrole-co-pyrrole) film, Sens. Actuators, B, 102 (2004) 271–277.
[36] S. Tembe, S. Inamdar, S. Harama, M. Karve, Electrochemical biosensor for catechol using agarose–guar gum entrapped tyrosinase, J. Biotechnol., 128 (2007) 80–85.
[37] B. Perez-Lopez, A. Merkoci, Magnetic nanoparticles modified with carbon nanotubes for electrocatalytic magneto switchable biosensing applications, Adv. Funct. Mater., 21 (2011) 255–260.
[38] A. Lorena, A. Gámez, M. Alonso-Lomillo, O. Domínguez-Renedo, M. Arcos-Martínez, A chronoamperometric screen printed carbon biosensor based on alkaline phosphatase inhibition for W(VI) determination in water, using 2-phospho-L-ascorbic acid trisodium salt as a substrate, Sensors, 15 (2015) 2232–2243.
[39] Q. Chen, S. Ai, X. Zhu, H. Yin, Q. Ma, Y. Qiu, A nitrite biosensor based on the immobilization of cytochrome C on multi-walled carbon nanotubes PAMAM-chitosan nanocomposite modified glass carbon electrode, Biosens. Bioelectron., 24 (2009) 2991–2996.